Cerebral Cortex July 2013;23:1526–1532
doi:10.1093/cercor/bhs135
Advance Access publication June 1, 2012

Impaired Language Pathways in Tuberous Sclerosis Complex Patients with Autism Spectrum Disorders

William W. Lewis[1,2], Mustafa Sahin[1], Benoit Scherrer[2], Jurriaan M. Peters[1,2], Ralph O. Suarez[2], Vanessa K. Vogel-Farley[3], Shafali S. Jeste[5], Matthew C. Gregas[1,4], Sanjay P. Prabhu[2], Charles A. Nelson, III[3] and Simon K. Warfield[2]

[1]Department of Neurology, [2]Department of Radiology, Computational Radiology Laboratory, [3]Laboratories of Cognitive Neuroscience, [4]Clinical Research Program, Children's Hospital Boston and Harvard Medical School, 300 Longwood Avenue, Boston, MA 02115, USA and [5]Center for Autism Research and Treatment, Semel Institute, University of California, 760 Westwood Plaza, Los Angeles, CA 90095, USA

*Address correspondence to Mustafa Sahin, Department of Neurology, Children's Hospital Boston and Harvard Medical School, 300 Longwood Avenue, Boston, MA 02115, USA. Email: mustafa.sahin@childrens.harvard.edu

The purpose of this study was to examine the relationship between language pathways and autism spectrum disorders (ASDs) in patients with tuberous sclerosis complex (TSC). An advanced diffusion-weighted magnetic resonance imaging (MRI) was performed on 42 patients with TSC and 42 age-matched controls. Using a validated automatic method, white matter language pathways were identified and microstructural characteristics were extracted, including fractional anisotropy (FA) and mean diffusivity (MD). Among 42 patients with TSC, 12 had ASD (29%). After controlling for age, TSC patients without ASD had a lower FA than controls in the arcuate fasciculus (AF); TSC patients with ASD had even a smaller FA, lower than the FA for those without ASD. Similarly, TSC patients without ASD had a greater MD than controls in the AF; TSC patients with ASD had even a higher MD, greater than the MD in those without ASD. It remains unclear why some patients with TSC develop ASD, while others have better language and socio-behavioral outcomes. Our results suggest that language pathway microstructure may serve as a marker of the risk of ASD in TSC patients. Impaired microstructure in language pathways of TSC patients may indicate the development of ASD, although prospective studies of language pathway development and ASD diagnosis in TSC remain essential.

Keywords: arcuate fasciculus, diffusion tensor imaging, neuroanatomy, tractography, white matter

Introduction

Tuberous sclerosis complex (TSC) is an autosomal-dominant neurocutaneous disease caused by the loss of either the *TSC1* (encoding hamartin) or *TSC2* (encoding tuberin) genes. TSC is characterized by lesions throughout the body, most commonly affecting the brain, kidneys, skin, and lungs (Crino et al. 2006).

Neurological symptoms are common in TSC and include epilepsy and behavioral conditions such as autism spectrum disorders (ASDs) (Crino et al. 2006). Between 17% and 61% of children with TSC exhibit ASD symptoms (Asano et al. 2001). Although cortical tubers seem to be related to epilepsy and may serve as foci for seizures, these tubers have a poorly defined relationship to neurocognitive deficits and to ASD in particular (Bolton et al. 2002; Walz et al. 2002; Curatolo et al. 2004; Jansen et al. 2008).

These neurological symptoms are likely interrelated. Jeste et al. (2008) found that TSC patients with ASD also exhibited significantly more general cognitive impairment than those without ASD. Nevertheless, many TSC patients without ASD had some cognitive impairment, and had deficits on the autism diagnostic observation schedule (ADOS). ASDs are common developmental disorders, with an estimated prevalence of 1 in 110 among children (Investigators 2007). Early indicators of ASD are extremely useful, because early intervention can significantly improve the expected outcome for most affected children (Filipek et al. 2000).

Neuroimaging allows for the early detection and characterization of brain abnormalities that may be useful for ASD diagnosis. It has already been used to characterize a variety of brain abnormalities in TSC patients, with a particular focus on the diffusion properties of cortical tubers (Asano et al. 2001). Nevertheless, despite considerable focus on tubers, the location, volume, and number of tubers do not correlate well with clinical variables of interest (Bolton et al. 2002; Curatolo et al. 2004; Wong and Khong 2006).

Instead, differences in the normal-appearing white matter (NAWM) may actually provide a better marker of neurological symptoms in TSC (Wakana et al. 2004; Makki et al. 2007; Peters et al. 2012). The differences in the NAWM of TSC patients have primarily been found in the white matter overall and in the corpus callosum specifically, raising the possibility of aberrant NAWM as a correlate of neurological deficits. Further supporting the relationship between NAWM and TSC, a recent report by Tillema et al. (2012) suggests that everolimus therapy can improve the white matter diffusion characteristics in TSC patients.

Diffusion tensor imaging (DTI) with tractography is a promising technique for delineating and analyzing white matter fiber pathways in living humans. DTI with tractography gives accurate and reproducible 3D representations of known connections (Mori et al. 1999; Ciccarelli et al. 2008). Water diffusion in the brain white matter can be described by microstructural variables, indicating the speed of the diffusion (mean diffusivity or MD) and the amount of directionality of the movement (fractional anisotropy or FA). Microstructural characteristics of the brain extracted from the DTI data describe changes in the brain due to development, traumatic injury, and disease processes (Song, Sun, Ramsbottom, et al. 2002; Song, Sun, Ju, et al. 2003).

The arcuate fasciculus (AF) is a crucial language pathway in the human brain connecting Broca's area in the frontal lobe to Wernicke's area in the temporal lobe. The AF has been validated by lesion studies and perioperative electrostimulation as essential for receptive and expressive language (Catani et al. 2005; Leclercq et al. 2010). Using tractography to analyze the AF, investigators have identified anomalies in a

variety of diseases, including idiopathic ASD (Fletcher et al. 2010), schizophrenia (de Weijer et al. 2011), Angelman syndrome (Wilson et al. 2011), and congenital bilateral perisylvian syndrome (Bernal et al. 2010), along with verifying its importance in normal language function (Lebel and Beaulieu 2009).

Work on schizophrenia by Catani et al. (2011) showed that examining the 3 segments of the AF can specify the portions associated with a particular clinical outcome (specifically auditory hallucinations). Previous work on idiopathic ASD (Fletcher et al. 2010; Knaus et al. 2010) suggested that the AF as a whole was modified in patients with ASD. We chose to investigate whether the changes in the AF were also found in TSC patients with ASD, as well as determining whether they were specific to a particular segment.

Thus, while white matter abnormalities have been identified in patients with TSC, and AF microstructure differences are associated with the variable neurological outcomes in several diseases, no studies have focused on the AF in TSC. Building from the studies connecting AF white matter integrity to a variety of pathologies, we examined a large group of TSC patients and age-matched controls. Since the TSC patients have variable ASD status, we asked whether microstructure changes in the AF were associated with ASD in this group of children.

Materials and Methods

Subjects

This study involved 42 patients (ages 0.5–25 years) diagnosed with TSC and 42 age-matched control subjects. All were imaged with 3 T MRI (Siemens Trio). Data from 6 of the age-matched controls were obtained with an identical acquisition protocol from collaborators at the University of North Carolina. The controls were either recruited specifically as healthy controls or were patients seen at the Children's Hospital Boston who received a clinical MRI for a reason other than TSC or developmental disability. A pediatric neuroradiologist reviewed each MRI; the clinical MRI for each control was found to be normal.

All 42 patients were diagnosed with definite TSC, as described by the Tuberous Sclerosis Consensus Conference (Roach et al. 1999). The TSC patients were followed in the Multidisciplinary Tuberous Sclerosis Program at Children's Hospital Boston. The ASD diagnosis were based on the clinical assessment by a board-certified pediatric neurologist (M.S. and S.S.J.) using the Diagnostic and Statistical Manual DSM-IV-TR, supplemented in all but the 3 oldest subjects with the ADOS (Lord et al. 2000) by experienced specialists (V.V.F. and S.S.J.). Recruitment of subjects, data acquisition, and data analysis were conducted with informed consent, using a protocol approved by the Institutional Review Board from the Children's Hospital Boston.

Data Acquisition and Analysis

Preprocessing

The MRI protocol included a routine clinical imaging and a diffusion imaging addition. Sedation was used for the clinical imaging if necessary to prevent excessive motion. The imaging protocol included a T1-weighted magnetization prepared rapid acquisition with gradient echo (MPRAGE) and a T2-weighted turbo spin echo, with diffusion imaging (Reese et al. 2003) acquired in the axial plane. The diffusion imaging comprised 30 slices with $b = 1000$ s/mm^2 and 5 $b = 0$ images. The intracranial cavity was segmented following the structural MRI (Grau et al. 2004; Weisenfeld and Warfield 2009). Diffusion images were aligned to the T1-weighted MPRAGE to compensate for distortion and patient motion (Ruiz-Alzola et al. 2002). We estimated the tensor fit with robust least-squares (Douek et al. 1991).

Tractography

We used a stochastic algorithm for tractography (Peters et al. 2012), combining the speed and accuracy of deterministic decision-making at each voxel with probabilistic sampling to better explore the space of all possible streamlines. Potential streamlines were stochastically initialized and evaluated starting from all white matter with a high FA (>0.4). Streamlines were constructed with sequential steps through the tensor field at sub-voxel resolution. While evaluating each streamline, we checked conventional stopping criteria, including streamline curvature and FA, but incorporated the prior path of the streamline to compensate for local inhomogeneities. Streamlines were estimated with log-Euclidean tensor interpolation (Arsigny et al. 2006) at each voxel, with a stepping direction determined by a linear combination of tensor deflection (Lazar et al. 2003) and primary eigenvector orientation. The range of potential streamlines examined is broad compared with conventional deterministic tractography. Stochastic sampling was continued until a predetermined number of streamlines had been created for each seed voxel.

Tract Selection

As proposed by Wakana et al. (2004), we specified regions-of-interests (ROIs) to ensure streamlines followed the known anatomy. We selected streamlines that ended near certain ROIs (selection ROIs), and excluded those that did pass through other ROIs (exclusion ROIs) to identify the 3 portions of the AF, following a previously validated procedure (Catani et al. 2005). Catani et al. use gray matter regions in Broca's area, Geschwind's territory, and Wernicke's area to define endpoints for the streamlines. Similarly, we defined 3 regions in the white matter adjacent to Broca's area, Geschwind's territory, and Wernicke's area to perform streamline selection. Figure 1 shows the selection method for the 3 segments of the AF, and Figure 2 shows the ROIs and 3 segments of the AF in selected subjects.

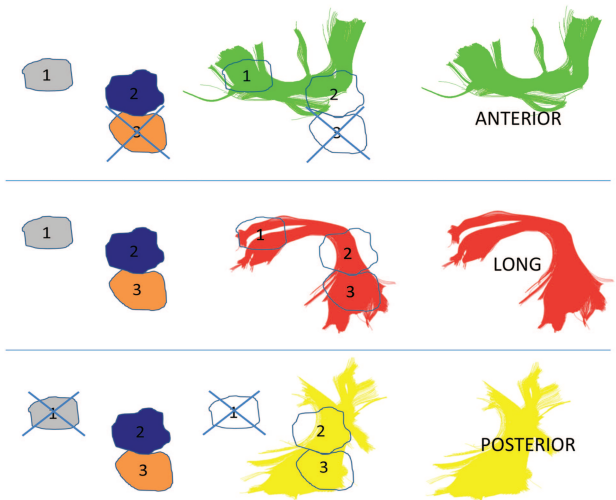

Figure 1. Schematic of the selection method for AF segments. Tracts shown are those for 1 control subject. Regions were automatically mapped onto all subjects, with region 1 in the white matter near Broca's territory, region 2 in the white matter near Geschwind's territory, and region 3 in the white matter near Wernicke's territory. The anterior segment was selected by choosing streamlines that passed through regions 1 and 2, but not region 3. The long segment was selected by choosing streamlines that passed through regions 1 and 3 (and which may pass through region 2 as well, but are not required to do so). The posterior segment was selected by choosing streamlines that passed through regions 2 and 3, but not region 1.

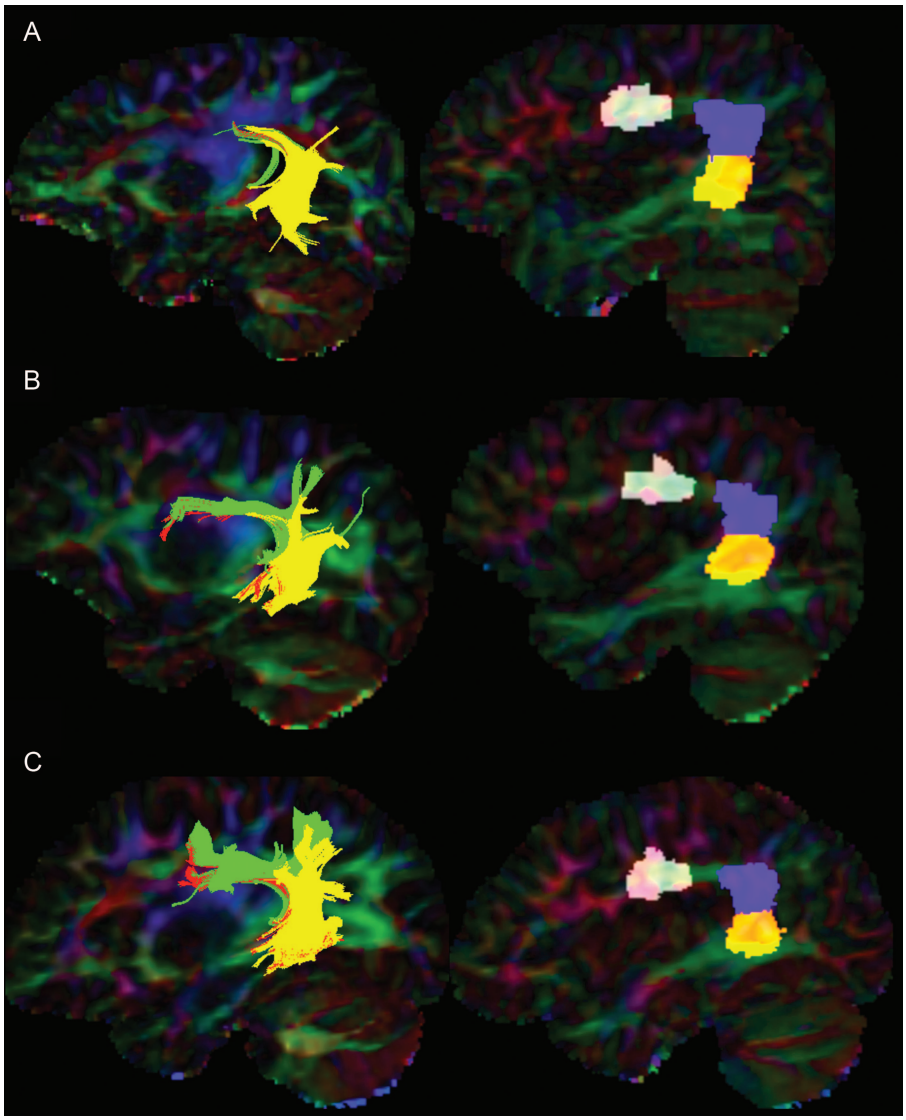

Figure 2. The segments of the AF and selection regions in patients and controls. Left side: segments of the AF in patients and controls. Green = anterior segment, red = long segment, yellow = posterior segment. Right side: ROIs used to select segments of AF. (*A*) A 13-year-old patient with ASD. (*B*) A 12-year-old patient without ASD. (*C*) A 12-year-old control subject. The ROIs and AF segments are superimposed on a color-map of the principal diffusion directions: green represents the anterior-to-posterior diffusion direction, blue superior to inferior, and red medial to lateral.

Extraction of Microstructural Data

The streamlines identified by stochastic tractography were then used to delineate an ROI for the assessment of white matter microstructural integrity. Voxels touched by <3% of the streamlines in the tract of interest were excluded from the analysis. Average parameters, including FA and MD, were assessed by computing the mean of each parameter for all voxels in the ROIs (Powell et al. 2006; Kubicki et al. 2011). Similarly, the volume of each tract was determined by summing the volume of all voxels touched by >3% of the streamlines within a tract of interest.

Generation of Selection ROIs

To automatically generate ROIs for a large number of subjects, we delineated each ROI in a set of 20 template brains. Using the STAPLE algorithm (Warfield et al. 2004), we mapped each ROI from the template brains onto each TSC patient and control subject, and selected the consensus voxels (Fig. 2 shows the ROIs mapped on the brains of selected subjects). This automatic mapping of ROIs eliminates potential human error or bias in selecting ROIs, as it can be done objectively across the various populations in our study (Suarez et al. 2012). For the template brains, the AF ROIs were delineated by inspection of the color-coded tensor image. Tracts in the subjects were selected using a multiple ROI approach (Catani et al. 2005). For statistical analysis, the FA and MD were derived from each tensor.

Statistical Analysis

The DTI microstructural measures were considered response variables in a regression model with age, sex, and group status. Three groups were examined: controls, TSC patients without ASD, and TSC patients without ASD. All 2-way interaction terms were considered, and terms were dropped from the model based on likelihood ratio tests and Akaike's information criteria (AIC). Only essential terms were retained to accurately characterize the data without extra predictors. A logarithmic transformation of age, log(age) was chosen rather than age based on a visual examination of the data and AIC. In the model, log(age) and group were significant predictors in each analysis for microstructural variables. Sex was a significant predictor in one of the analyses. The level of significance (α) was set at 0.05. Different models were fit

Table 1
The logistic regression models for each segment (anterior, long, and posterior) and microstructural variable (FA and MD)

	Controls (age 1)	Log(age)	Sex	Patients without ASD	Patients with ASD	Patients without ASD × log(age)	Patients with ASD × log(age)	Patients without ASD × sex	Patients with ASD × sex
Anterior segment									
FA	0.366	0.0361***		−0.0189	−0.0485*** ‡				
MD	8.32E-04	−4.98E-05***		2.32E-05	−5.73E-05	5.75E-06	5.77E-05* ‡		
Long segment									
FA	0.375	0.0363***		−0.0227*	−0.0602*** ‡				
MD	8.90E-04	−5.10E-05***		3.25E-05*	1.07E-04*** ‡‡‡				
Posterior segment									
FA	0.366	0.0318***		−0.0226*	−0.0512*** ‡				
MD	9.32E-04	−6.72E-05***	5.99E-05	1.38E-04**	6.868E-05			−7.31E-05*	4.76E-05

The first column shows the baseline condition, a male control subject at age 1. Each additional column shows the β-value from the regression model for the indicated variable. The β-value reflects the modification of the baseline value for each variable in the regression. Significant differences are noted. The best models for FA and MD incorporate only the natural logarithm of the age and group membership, with the exception of the posterior segment MD, which also includes sex in the best model. There are 2 different markers for significance.
For comparisons to controls: $^{*}P < 0.05$; $^{**}P < 0.01$; and $^{***}P < 0.001$. Both TSC patients without ASD and with ASD were compared with controls.
For comparisons to patients without ASD: $^{\ddagger}P < 0.05$; $^{\ddagger\ddagger}P < 0.01$; and $^{\ddagger\ddagger\ddagger}P < 0.001$. In a separate statistical test, TSC patients with ASD were compared with those without ASD.

for each microstructural variable (FA and MD) and each segment of the AF (anterior, long, and posterior).

Results

Patients

Forty-two subjects (28 boys, 14 girls; mean age 9.9 years; age range 1–27 years, median age 8.6 years) underwent diffusion-weighted MRI. Forty-two age-matched controls (20 boys, 22 girls; mean age 9.9 years; age range 1–25 years, median age 8.7 years) with clinically normal MRIs were also included.

Microstructural Characteristics of the Arcuate Fasciculus

Table 1 presents the multiple regression models describing the changes in microstructural variables (FA and MD) with age for each segment (anterior, long, and posterior) and each group (controls, patients without ASD, and patients with ASD). There were no differences in the volume of the AF between controls and TSC patients without ASD or between controls and TSC patients with ASD.

Anterior Segment

Fractional anisotropy

For the mean FA in the anterior segment of the AF, we compared groups while controlling for age. The controls and TSC patients without ASD are not significantly different ($P = 0.062$), while there is a large difference in FA between controls and TSC patients with ASD ($P = 0.00084$). The FA of TSC patients without ASD is also larger than the FA of TSC patients with ASD ($P = 0.047$; Fig. 4).

Mean diffusivity

For the mean MD, the response in each group is modified by age. In particular, the MD decreases with age more quickly in controls than in TSC patients with ASD ($P = 0.011$), but does not decrease more quickly in controls than in TSC patients without ASD. The MD also decreases with age more quickly in TSC patients without ASD than those with ASD ($P = 0.033$).

Long Segment

Fractional anisotropy

For the mean FA in the long segment of the AF, we again compared groups while controlling for age. The controls and TSC patients without ASD are different, although the difference is small ($P = 0.045$). There is a large difference, however, between the controls and TSC patients with ASD ($P = 0.00017$); controls have a much higher FA at each age. TSC patients without ASD also have a significantly higher FA than those with ASD ($P = 0.021$). Figure 4 shows a comparison of the predicted FA at age one for each group.

Mean diffusivity

Similarly, for the MD and after controlling for age, we found a small significant difference between controls and TSC patients without ASD ($p = 0.026$), but a very large difference between controls and TSC patients with ASD ($P < 0.0001$). Controls have a much lower MD at each age. TSC patients without ASD also have a significantly lower MD than those with ASD ($P = 0.00047$). Figure 3 shows the progression of MD by age in the long segment for each group.

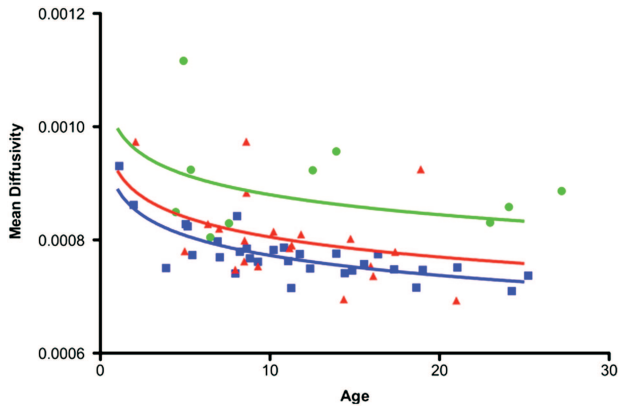

Figure 3. The long segment MD progression by age. Controls (blue) have a lower MD at all ages than patients without ASD (red), and patients with ASD (green). Controls have a lower MD than patients without ASD, although the difference is small ($P = 0.026$). Controls have a much lower MD than patients with ASD ($P < 0.000001$). Patients without ASD also have a much lower MD than those with ASD ($P = 0.0005$).

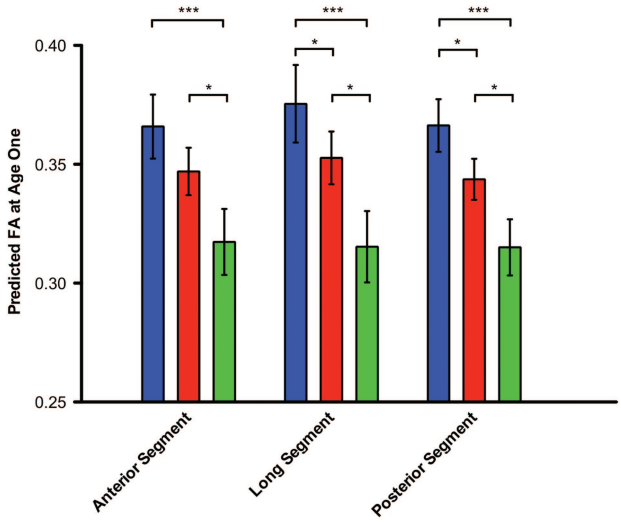

Figure 4. The predicted FA values at age 1 for controls and patients. The predicted FA values at age 1 for controls (blue), patients without ASD (red), and patients with ASD (green). The predicted FA values at age 1 do not reflect a set of patients at age 1, but rather are predictions of the FA at age 1 based on the regression models for the 3 groups. For the anterior segment, only the patients with ASD have a different FA from controls ($P = 0.00082$). The patients with ASD also have a significantly lower FA than those without ASD ($P = 0.047$). For the long segment, the controls are significantly different from both patients without ASD ($P = 0.045$) and with ASD ($P = 0.00017$). The patients with ASD again had a significantly lower FA than those without ASD ($P = 0.02$). Similarly, for the posterior segment, control FA values are different from patients without ASD ($P = 0.010$) and with ASD ($P = 0.000045$). Patients with ASD had a significantly lower FA than those without ASD ($P = 0.02$). Error bars represent standard error of the intercept from the regression analysis. $^*P < 0.05$; $^{***}P < 0.001$.

Posterior Segment

Fractional anisotropy

Finally, for the mean FA in the posterior segment of the AF, we examined the 3 groups while controlling for age. As before, the controls and TSC patients without ASD had modest, but significantly different values ($P = 0.010$), while controls and TSC patients with ASD had very different FA values ($P < 0.0001$). TSC patients without ASD also had higher FA than those with ASD ($P = 0.024$; see Fig. 4).

Mean diffusivity

For the MD, we again examined the 3 groups while controlling for age. Sex modified the effect of ASD diagnosis on the results. In particular, there was a significant difference between males and females in the group of patients without ASD, a difference that was not found in other segments or for other measures in the AF. TSC patients without ASD had higher MD than controls overall ($P = 0.0041$), but female TSC patients without ASD had lower MD than male TSC patients without ASD ($P = 0.017$).

Discussion

This paper is the first examining microstructural characteristics of language pathways in TSC. Moreover, it is only the second analysis of TSC brain diffusion microstructure of any region that also incorporates the clinical neurological outcome, following a recent study on the corpus callosum (Peters et al. 2012). An earlier study by Ridler et al. (2007) provided the first evidence that neuroanatomical changes in TSC patients correlate with clinical variables, relating abnormalities in the gray and white matter volume with memory function. Other work on TSC has been unable to examine neurological correlates of neuroimaging findings due to a smaller sample size. The decreased FA in patients relative to controls—and particularly in patients with ASD—in all 3 segments of the AF suggests that TSC is associated with impaired tract cohesion in language regions of the brain. A decreased FA indicates poor tract integrity and likely represents diminished compactness of the fiber tracts. The developmental trajectories of microstructural variables appear similar across groups, but the model suggests that the FA is significantly different at age one (represented by the intercepts of the log (age) fits, Fig. 4). This difference in early FA appears to be maintained through development, potentially relating to the high prevalence of language deficits in the TSC population.

Similarly, increased MD in patients, particularly those with ASD, suggests impaired maturation of white matter language pathways. A higher MD in the TSC population may be related to incomplete or improper myelination compared with normal controls (Song, Sun, Ramsbottom, et al. 2002; Song, Sun, Ju, et al. 2003). Improper or inadequate myelination in TSC is consistent with mouse studies demonstrating reduced myelination in the brains of mice lacking *Tsc1* or *Tsc2* (Meikle et al. 2007; Way et al. 2009). Nevertheless, mutations in *TSC1* and *TSC2* cause a variety of neural abnormalities in mouse models, including changes in neurofilaments and cell size, as well as dendritic spine density and length. Thus, although hypomyelination may be partly responsible for the observed increase in MD in TSC patients, more general neuronal dysfunction likely contributes as well.

It is somewhat surprising that changes in the volume of the AF were not seen in patients with TSC. The aberrant development of language pathways in this patient group might be expected to contribute to the volume changes as well. Fletcher et al. (2010) found results similar to us in patients with high-functioning autism. They observed no volume changes with age, and no volume differences between patients with ASD and controls. Some evidence, though, suggests that subjects with typical language activation actually have a lower volume of the AF (Knaus et al. 2010).

Nevertheless, these results are consistent with the findings of aberrant AF structure in the idiopathic ASD. A recent work suggests that the microstructure of the AF is modified in patients with high-functioning ASD compared with age-matched controls, even when controlling for overall white matter microstructure (Fletcher et al. 2010). Patients with ASD are also more likely to have atypical laterality than controls, although there were subjects with atypical laterality in both groups (Knaus et al. 2010).

It is also challenging to explain why the different segments show varying results. In this study, the long segment showed the largest differences among the groups, while the microstructure of the anterior and posterior segments was more similar across the groups. These results suggest that the long segment may be more selective for language differences in TSC than the anterior and posterior segments of the AF. The long segment represents the traditional AF that has been validated in previous studies of language and in ASD (Lebel and Beaulieu 2009; Fletcher et al. 2010; Knaus et al. 2010) and overlaps with both the anterior and the posterior segments.

The microstructural differences among groups in the anterior and posterior segments may be due to those portions that overlap with the long segment, while the non-overlapping regions may be more similar across the 3 groups.

The results must be considered in the setting of several limitations. First, no continuous language or intelligence measure was collected on this clinical sample of TSC patients. A continuous language or intelligence measure would have allowed us to more closely examine the relationship between the AF microstructure and developmental outcome in the TSC population as a whole. Prospective studies using continuous language measures are in progress. Secondly, we identified groups based on ASD diagnosis. There may be other developmental differences between these groups that we have not identified. Future studies with larger numbers of subjects may be able to find these. Thirdly, while DTI tractography has been used to study a number of neurological illnesses (Ciccarelli et al. 2008; Fletcher et al. 2010; Knaus et al. 2010; de Weijer et al. 2011), it does not directly examine functional connections in the brain. Instead, DTI tractography outlines the likely pathways of axon bundles, but may not precisely trace the route of language information in the brain.

Thus, our findings demonstrate that controls, TSC patients without ASD, and TSC patients with ASD at a given age have significantly different AF microstructure. The differences are particularly pronounced when comparing controls and TSC patients with ASD. Recent work has also correlated ASD in TSC to early seizure activity and more frequent seizures (Numis et al. 2011). It is unclear, though, whether ASD and frequent/early seizures have a common cause, or whether the seizures themselves may cause autistic symptoms directly.

The results from this study, particularly the model suggesting poor AF microstructural integrity from age one, indicate a possible relationship among aberrant white matter microstructural integrity, poor cognitive function, early seizures, and ASD. While the group of ASD patients, in general, is heterogeneous, studying TSC patients can help shed light on patients with ASD caused by genetic defects in *TSC1/2* and genes in related molecular pathways (Tsai and Sahin 2011).

Funding

This work was supported by the John Merck Fund and a Junior Investigator Award from the Children's Hospital Boston Translational Research Program to M.S., an award from the Children's Hospital Boston Translational Research Program to S.K.W., and the National Institutes of Health (R01 DC010290 to C.A.N. III; RO1 RR021885, R01 LM01033, and R03 EB008680 to S.K.W.).

Notes

The authors first acknowledge the generous and essential contributions of the children and families who participated in this study. We also gratefully acknowledge the contribution of MRI scans from John Gilmore and Martin Styner of the University of North Carolina – Chapel Hill. Their work was supported by NIH grant P50 MH064065. *Conflict of Interest:* None declared.

References

Arsigny V, Fillard P, Pennec X, Ayache N. 2006. Log-Euclidean metrics for fast and simple calculus on diffusion tensors. Magn Reson Med. 56:411–421.

Asano E, Chugani DC, Muzik O, Behen M, Janisse J, Rothermel R, Mangner TJ, Chakraborty PK, Chugani HT. 2001. Autism in tuberous sclerosis complex is related to both cortical and subcortical dysfunction. Neurology. 57:1269–1277.

Bernal B, Rey G, Dunoyer C, Shanbhag H, Altman N. 2010. Agenesis of the arcuate fasciculi in congenital bilateral perisylvian syndrome: a diffusion tensor imaging and tractography study. Arch Neurol. 67:501–505.

Bolton PF, Park RJ, Higgins JN, Griffiths PD, Pickles A. 2002. Neuro-epileptic determinants of autism spectrum disorders in tuberous sclerosis complex. Brain. 125:1247–1255.

Catani M, Craig MC, Forkel SJ, Kanaan R, Picchioni M, Toulopoulou T, Shergill S, Williams S, Murphy DG, McGuire P. 2011. Altered integrity of perisylvian language pathways in schizophrenia: relationship to auditory hallucinations. Biol Psychiatry. 70:1143–1150.

Catani M, Jones DK, Ffytche DH. 2005. Perisylvian language networks of the human brain. Ann Neurol. 57:8–16.

Ciccarelli O, Catani M, Johansen-Berg H, Clark C, Thompson A. 2008. Diffusion-based tractography in neurological disorders: concepts, applications, and future developments. Lancet Neurol. 7:715–727.

Crino PB, Nathanson KL, Henske EP. 2006. The tuberous sclerosis complex. N Engl J Med. 355:1345–1356.

Curatolo P, Porfirio MC, Manzi B, Seri S. 2004. Autism in tuberous sclerosis. Eur J Paediatr Neurol. 8:327–332.

de Weijer AD, Mandl RC, Diederen KM, Neggers SF, Kahn RS, Hulshoff Pol HE, Sommer IE. 2011. Microstructural alterations of the arcuate fasciculus in schizophrenia patients with frequent auditory verbal hallucinations. Schizophr Res. 130:68–77.

Douek P, Turner R, Pekar J, Patronas N, Le Bihan D. 1991. MR color mapping of myelin fiber orientation. J Comput Assist Tomogr. 15:923–929.

Filipek PA, Accardo PJ, Ashwal S, Baranek GT, Cook EH, Jr, Dawson G, Gordon B, Gravel JS, Johnson CP, Kallen RJ *et al.* 2000. Practice parameter: screening and diagnosis of autism: report of the Quality Standards Subcommittee of the American Academy of Neurology and the Child Neurology Society. Neurology. 55:468–479.

Fletcher PT, Whitaker RT, Tao R, DuBray MB, Froehlich A, Ravichandran C, Alexander AL, Bigler ED, Lange N, Lainhart JE. 2010. Microstructural connectivity of the arcuate fasciculus in adolescents with high-functioning autism. Neuroimage. 51:1117–1125.

Grau V, Mewes AU, Alcaniz M, Kikinis R, Warfield SK. 2004. Improved watershed transform for medical image segmentation using prior information. IEEE Trans Med Imaging. 23:447–458.

Investigators AaDDMNSYP. 2007. Prevalence of autism spectrum disorders—autism and developmental disabilities monitoring network, 14 sites, United States, 2002. MMWR Surveill Summ. 56:12–28.

Jansen FE, Vincken KL, Algra A, Anbeek P, Braams O, Nellist M, Zonnenberg BA, Jennekens-Schinkel A, van den Ouweland A, Halley D *et al.* 2008. Cognitive impairment in tuberous sclerosis complex is a multifactorial condition. Neurology. 70:916–923.

Jeste SS, Sahin M, Bolton P, Ploubidis GB, Humphrey A. 2008. Characterization of autism in young children with tuberous sclerosis complex. J Child Neurol. 23:520–525.

Knaus TA, Silver AM, Kennedy M, Lindgren KA, Dominick KC, Siegel J, Tager-Flusberg H. 2010. Language laterality in autism spectrum disorder and typical controls: a functional, volumetric, and diffusion tensor MRI study. Brain Lang. 112:113–120.

Kubicki M, Alvarado JL, Westin CF, Tate DF, Markant D, Terry DP, Whitford TJ, De Siebenthal J, Bouix S, McCarley RW *et al.* 2011. Stochastic tractography study of Inferior Frontal Gyrus anatomical connectivity in schizophrenia. Neuroimage. 55:1657–1664.

Lazar M, Weinstein DM, Tsuruda JS, Hasan KM, Arfanakis K, Meyerand ME, Badie B, Rowley HA, Haughton V, Field A *et al.* 2003. White matter tractography using diffusion tensor deflection. Hum Brain Mapp. 18:306–321.

Lebel C, Beaulieu C. 2009. Lateralization of the arcuate fasciculus from childhood to adulthood and its relation to cognitive abilities in children. Hum Brain Mapp. 30:3563–3573.
Leclercq D, Duffau H, Delmaire C, Capelle L, Gatignol P, Ducros M, Chiras J, Lehericy S. 2010. Comparison of diffusion tensor imaging tractography of language tracts and intraoperative subcortical stimulations. J Neurosurg. 112:503–511.
Lord C, Risi S, Lambrecht L, Cook EH, Jr, Leventhal BL, DiLavore PC, Pickles A, Rutter M. 2000. The autism diagnostic observation schedule-generic: a standard measure of social and communication deficits associated with the spectrum of autism. J Autism Dev Disord. 30:205–223.
Makki MI, Chugani DC, Janisse J, Chugani HT. 2007. Characteristics of abnormal diffusivity in normal-appearing white matter investigated with diffusion tensor MR imaging in tuberous sclerosis complex. AJNR Am J Neuroradiol. 28:1662–1667.
Meikle L, Talos DM, Onda H, Pollizzi K, Rotenberg A, Sahin M, Jensen FE, Kwiatkowski DJ. 2007. A mouse model of tuberous sclerosis: neuronal loss of Tsc1 causes dysplastic and ectopic neurons, reduced myelination, seizure activity, and limited survival. J Neurosci. 27:5546–5558.
Mori S, Crain BJ, Chacko VP, van Zijl PC. 1999. Three-dimensional tracking of axonal projections in the brain by magnetic resonance imaging. Ann Neurol. 45:265–269.
Numis AL, Major P, Montenegro MA, Muzykewicz DA, Pulsifer MB, Thiele EA. 2011. Identification of risk factors for autism spectrum disorders in tuberous sclerosis complex. Neurology. 76:981–987.
Peters JM, Sahin M, Vogel-Farley VK, Jeste SS, Nelson CA, 3rd, Gregas MC, Prabhu SP, Scherrer B, Warfield SK. 2012. Loss of white matter microstructural integrity is associated with adverse neurological outcome in tuberous sclerosis complex. Acad Radiol. 19:17–25.
Powell HW, Parker GJ, Alexander DC, Symms MR, Boulby PA, Wheeler-Kingshott CA, Barker GJ, Noppeney U, Koepp MJ, Duncan JS. 2006. Hemispheric asymmetries in language-related pathways: a combined functional MRI and tractography study. Neuroimage. 32:388–399.
Reese TG, Heid O, Weisskoff RM, Wedeen VJ. 2003. Reduction of eddy-current-induced distortion in diffusion MRI using a twice-refocused spin echo. Magn Reson Med. 49:177–182.
Ridler K, Suckling J, Higgins NJ, de Vries PJ, Stephenson CM, Bolton PF, Bullmore ET. 2007. Neuroanatomical correlates of memory deficits in tuberous sclerosis complex. Cereb Cortex. 17:261–271.
Roach ES, DiMario FJ, Kandt RS, Northrup H. 1999. Tuberous Sclerosis Consensus Conference: recommendations for diagnostic evaluation. National Tuberous Sclerosis Association. J Child Neurol. 14:401–407.
Ruiz-Alzola J, Westin CF, Warfield SK, Alberola C, Maier S, Kikinis R. 2002. Nonrigid registration of 3D tensor medical data. Med Image Anal. 6:143–161.
Song SK, Sun SW, Ju WK, Lin SJ, Cross AH, Neufeld AH. 2003. Diffusion tensor imaging detects and differentiates axon and myelin degeneration in mouse optic nerve after retinal ischemia. Neuroimage. 20:1714–1722.
Song SK, Sun SW, Ramsbottom MJ, Chang C, Russell J, Cross AH. 2002. Dysmyelination revealed through MRI as increased radial (but unchanged axial) diffusion of water. Neuroimage. 17:1429–1436.
Suarez RO, Commowick O, Prabhu SP, Warfield SK. 2012. Automated delineation of white matter fiber tracts with a multiple region-of-interest approach. NeuroImage. 59:3690–3700.
Tillema JM, Leach JL, Krueger DA, Franz DN. 2012. Everolimus alters white matter diffusion in tuberous sclerosis complex. Neurology. 78:526–531.
Tsai P, Sahin M. 2011. Mechanisms of neurocognitive dysfunction and therapeutic considerations in tuberous sclerosis complex. Curr Opin Neurol. 24:106–113.
Wakana S, Jiang H, Nagae-Poetscher LM, van Zijl PC, Mori S. 2004. Fiber tract-based atlas of human white matter anatomy. Radiology. 230:77–87.
Walz NC, Byars AW, Egelhoff JC, Franz DN. 2002. Supratentorial tuber location and autism in tuberous sclerosis complex. J Child Neurol. 17:830–832.
Warfield SK, Zou KH, Wells WM. 2004. Simultaneous truth and performance level estimation (STAPLE): an algorithm for the validation of image segmentation. IEEE Trans Med Imaging. 23:903–921.
Way SW, McKenna J, 3rd, Mietzsch U, Reith RM, Wu HC, Gambello MJ. 2009. Loss of Tsc2 in radial glia models the brain pathology of tuberous sclerosis complex in the mouse. Hum Mol Genet. 18:1252–1265.
Weisenfeld NI, Warfield SK. 2009. Automatic segmentation of newborn brain MRI. Neuroimage. 47:564–572.
Wilson BJ, Sundaram SK, Huq AH, Jeong JW, Halverson SR, Behen ME, Bui DQ, Chugani HT. 2011. Abnormal language pathway in children with Angelman syndrome. Pediatr Neurol. 44:350–356.
Wong V, Khong PL. 2006. Tuberous sclerosis complex: correlation of magnetic resonance imaging (MRI) findings with comorbidities. J Child Neurol. 21:99–105.